

# Hybrid Memetic Search for Electric Vehicle Routing with Time Windows, Simultaneous Pickup-Delivery, and Partial Recharges

Zubin Zheng, Shengcai Liu, *Member, IEEE*, and Yew-Soon Ong, *Fellow, IEEE*

**Abstract**—With growing environmental concerns, electric vehicles for logistics have gained significant attention within the computational intelligence community in recent years. This work addresses an emerging and significant extension of the electric vehicle routing problem (EVRP), namely EVRP with time windows, simultaneous pickup-delivery, and partial recharges (EVRP-TW-SPD), which has wide real-world applications. We propose a hybrid memetic algorithm (HMA) for solving EVRP-TW-SPD. HMA incorporates two novel components: a parallel-sequential station insertion procedure for handling partial recharges that can better avoid local optima compared to purely sequential insertion, and a cross-domain neighborhood search that explores solution spaces of both electric and non-electric problem domains simultaneously. These components can also be easily applied to various EVRP variants. To bridge the gap between existing benchmarks and real-world scenarios, we introduce a new, large-scale EVRP-TW-SPD benchmark set derived from real-world applications, containing instances with many more customers and charging stations than existing benchmark instances. Extensive experiments demonstrate the significant performance advantages of HMA over existing algorithms across a wide range of problem instances. Both the benchmark set and HMA will be open-sourced to facilitate further research in this area.

**Index Terms**—Electric vehicle routing problem, memetic algorithm, combinatorial optimization, real-world application.

## I. INTRODUCTION

OVER the past few decades, the vehicle routing problem (VRP) has drawn much attention in the computational intelligence community [1]–[3], due to its extensive real-world applications. As VRP research moves forward, a new focus has emerged: the electric vehicle routing problem (EVRP) [4]. This area has gained a lot of interest in recent years, as more and more electric vehicles (EVs) are being used in various sectors [5]–[7], such as public transit, home deliveries, postal services, distribution tasks, and emergency power supply. While EVs enable zero-emission logistics, operating a fleet of EVs presents additional challenges compared to operating conventional vehicles: i) the lower energy density of batteries compared to the fuel of combustion engine vehicles, necessitating EVs to perform longer detours to recharge batteries;

ii) the limited number of public charging stations; and iii) the substantial time required for battery charging. To address these challenges, Erdogan and Miller-Hooks [8] introduced the first EVRP model that incorporated charging stations, as part of their broader study on the green VRP (G-VRP). Built on their work, subsequent studies have progressively incorporated more constraints into EVRP models to reflect real-world scenarios [9], [10].

This work focuses on an emerging and significant extension of EVRP, namely the electric vehicle routing problem with time windows, simultaneous pickup-delivery, and partial recharges (EVRP-TW-SPD), introduced by Akbay *et al.* [11]. Compared to the basic EVRP model, EVRP-TW-SPD considers more realistic problem characteristics and constraints, encompassing a wider range of real-world scenarios. Specifically, this model includes constraints such as limited driving range that requires en route recharging and strict customer service time windows [12]. Additionally, it incorporates two key characteristics: reverse logistics and partial recharges. In reverse logistics [13], [14], customers have both pickup and delivery demands, requiring EVs to complete both services in one trip. Partial recharges [15], [16] mean that EVs are not necessarily fully charged each time they visit a charging station, saving time to serve customers with tight time windows.

Despite the extensive real-world applications of EVRP-TW-SPD, current research in this area remains limited [11], [17], [18]. Specifically, existing approaches for solving EVRP-TW-SPD can be categorized into approximation methods [18] and metaheuristic methods [11], [17]. However, neither approach has shown fully satisfactory performance. Our experiments reveal that even for medium-scale instances with around 100 customers, there is significant room for improvement in solution quality obtained by existing methods. Furthermore, there is a notable gap between the scale of existing benchmark instances and real-world scenarios. The largest instance in the publicly available benchmark [11] contains only 100 customers and 21 charging stations. In contrast, with the rapid growth of urban areas, a real-world EVRP-TW-SPD instance might involve many more customers and stations [19], [20]. For example, application data from JD Logistics in Beijing<sup>1</sup>, a major city in China, shows scenarios with up to 1000 customers and 100 charging stations. This disparity highlights the need for establishing larger-scale benchmarks to drive research that better addresses practical challenges.

Zubin Zheng and Shengcai Liu are with the Department of Computer Science and Engineering, Southern University of Science and Technology, Shenzhen, China. Email: zhengzb2021@mail.sustech.edu.cn; liusc3@sustech.edu.cn

Yew-Soon Ong is with the Centre for Frontier AI Research (CFAR), Agency for Science, Technology and Research (A\*STAR), Singapore, and is also with the College of Computing and Data Science, Nanyang Technological University (NTU), Singapore. Email: asysong@ntu.edu.sg

This work was partially conducted during Zubin’s internship at CFAR.

<sup>1</sup>JD Logistics is one of the largest logistics companies in China.

This work aims to address the above research limitations. Specifically, we propose a novel hybrid memetic algorithm (HMA) for solving EVRP-TW-SPD. HMA combines individual-based large neighborhood search with population-based memetic search, leveraging their complementary strengths to quickly find high-quality solutions and further improve solution quality. Importantly, HMA introduces two key novelties. First, it incorporates a parallel-sequential station insertion procedure (PSSI) for handling partial recharges. Compared to the sequential station insertion procedure commonly used in the literature [15], [21], [22], PSSI can better avoid local optima and construct higher-quality routes with acceptable additional computational cost. Second, HMA employs a cross-domain neighborhood search (CDNS) as its local search module. CDNS simultaneously explores two different neighborhoods: those of the non-electric counterpart of EVRP-TW-SPD (i.e., VRP-TW-SPD) and EVRP-TW-SPD itself. This expanded search space not only leads to higher-quality solutions but also allows for easy reuse of efficient local search procedures from non-electric VRP variants, which are often more extensively studied. Finally, to address the gap in the scale of benchmark instances, we propose a new benchmark set based on real customer data from JD Logistics in the central area of Beijing.

The main contributions of this work are summarized below.

- 1) We propose a novel hybrid memetic algorithm (HMA) for solving EVRP-TW-SPD. HMA integrates two novel components: PSSI for handling partial recharges and CDNS as the local search module. We further discuss the potential of applying them to a wide range of EVRP variants beyond EVRP-TW-SPD.
- 2) We introduce a new, large-scale EVRP-TW-SPD benchmark set derived from real-world applications. This set, which will be made open-source, contains instances with up to 1000 customers and 100 charging stations, aiming to drive research in the field.
- 3) Extensive experiments validate the effectiveness of HMA, demonstrating its significant performance advantage over existing methods across a wide range of problem instances.

The rest of this paper is organized as follows. Section II presents a literature review. Section III formally defines the problem. Section IV first describes the novel components of HMA, followed by the hybrid framework. Section V compares the proposed algorithm against existing methods using the existing benchmark and introduces the new benchmark. Finally, Section VI concludes the paper.

## II. RELATED WORK

In this section, we first review literature related to two key aspects of EVRP-TW-SPD: reverse logistics and partial recharges, followed by existing methods for the problem.

Reverse logistics, which involves the bi-directional flow of goods in pickup and delivery, is crucial in modern transportation due to its importance in satisfying distinct customer demands and lowering energy consumption. According to [23], the VRPs involving reverse logistics have often been referred

to as pickup and delivery problems (PDPs). Among PDPs, the VRP with simultaneous pickup-delivery (VRPSPD) is the most studied variant [24], [25], where vehicles deliver goods from a central depot to customers while also picking up items from customers to return to the depot. VRPSPD was first studied in [26] for a book distribution system with 22 customers and two vehicles, demonstrating that combining pickup and delivery operations leads to significant savings in time and distance compared to separate operations. Since then, numerous studies have been conducted on VRPSPD and its variants. In EVRP-TW-SPD, to handle simultaneous pickup-delivery, existing techniques from VRPSPD research [13], [27], [28] can be adapted. Specifically, in this work we integrate the residual capacity and radical surcharge (RCRS) [13] construction heuristic into the HMA algorithm.

Compared to full recharges, partial recharges are a more realistic and practical charging scheme in the real world. It allows for flexible charging time, which can help EVs meet tight time windows and potentially serve more customers. To handle partial recharges, two key aspects need to be considered: station selection and charge amount calculation. First, station selection refers to choosing which charging station EVs should use when they need to recharge. Most existing approaches for station selection rely on heuristic insertion strategies. Some approaches, like those in [29], [30], focus on minimizing the distance from the current customer to the nearest charging station. Others, such as [11], [15], [17], [31], aim to minimize the increase in total distance caused by inserting a charging station. Specifically, Keskin *et al.* [15] proposed three station insertion heuristics: greedy station insertion, greedy station insertion with comparison, and best station insertion. In contrast, Wang *et al.* [20] took a different approach by minimizing a generalized cost function that includes the objective function, time window, and distance violations. Second, charge amount calculation involves determining how much to recharge at each charging station. Several approaches have been proposed. Felipe *et al.* [32] suggested charging only the minimum amount needed to reach the next charging station or depot. Keskin *et al.* [15] ensured sufficient charge to reach the next station or depot while adjusting for time window constraints. They also found that partial recharges perform significantly better than full recharges, even with pre-determined charging amounts. Desaulniers *et al.* [16] and Wang *et al.* [20] considered both the minimum required charge and available slack time when determining charge amount. Similar to [16], [20], our approach for determining charge amount also considers both the minimal required charge and available slack time, ensuring sufficient battery state while meeting all time constraints.

Currently, research on EVRP-TW-SPD is still rather limited. Akbay *et al.* [11] introduced the problem and formulated it as a mixed integer linear programming (MILP) model. They proposed a metaheuristic approach called Adapt-CMSA-STD and compared it with CPLEX and other heuristics on instances with up to 100 customers and 21 charging stations. Their follow-up work [17] presented Adapt-CMSA-SETCOV, which used vehicle-route representations and a set-covering-based MILP model and showed performance improvement

over Adapt-CMSA-STD. Feng *et al.* [18] developed an alternating direction multiplier method for EVRP-TW-SPD with full recharges, testing it on small-scale instances with up to 15 customers and 6 charging stations.

### III. NOTATIONS AND PROBLEM DEFINITION

Formally, the EVRP-TW-SPD is defined on a complete directed graph  $\mathbf{G} = (\mathbf{V}', \mathbf{E})$ , where  $\mathbf{V}' = \{0\} \cup \mathbf{V} \cup \mathbf{F} = \{0, 1, 2, \dots, M + P\}$  is the node set. Here, 0 represents the depot,  $\mathbf{V} = \{1, 2, \dots, M\}$  is a set of  $M$  customers, and  $\mathbf{F} = \{M + 1, \dots, M + P\}$  is a set of  $P$  charging stations allowing multiple visits. The arc set  $\mathbf{E} = \{(i, j) \mid i, j \in \mathbf{V}', i \neq j\}$  is defined between each pair of nodes. Each node  $i \in \mathbf{V}'$  has five attributes: delivery demand  $u_i$ , pickup demand  $v_i$ , time window  $[e_i, l_i]$ , and service time  $s_i$ . For a customer  $i$ ,  $u_i$  is the amount of goods delivered from the depot, and  $v_i$  is the amount of goods picked up to be returned to the depot. The time window  $[e_i, l_i]$  defines the earliest and latest time for customer service, with arrivals before  $e_i$  resulting in waiting and after  $l_i$  being infeasible.  $s_i$  is the unloading/loading time at customer  $i$ . For the depot 0,  $e_0$  and  $l_0$  are the earliest departure and latest return time for EVs, respectively, with  $u_0 = v_0 = s_0 = 0$ . For a charging station  $i \in \mathbf{F}$ ,  $u_i = v_i = s_i = 0$ , and  $e_i = e_0$ ,  $l_i = l_0$ . Each arc  $(i, j) \in \mathbf{E}$  is associated with a travel distance  $d_{ij}$  and a travel time  $t_{ij}$ .

A homogeneous fleet of EVs, all with identical loading capacity  $C$ , battery capacity  $Q$ , and dispatching cost  $\mu_1$ , is initially located at the depot. The EVs depart from the depot, serve customers, and finally return to the depot. When an EV visits a charging station, its battery is recharged at a constant rate of  $g > 0$ , i.e., it takes time  $g$  to charge one unit of battery energy. Conversely, the constant  $h$  represents the EV's battery energy consumption rate per unit of travel distance for the EV.

A solution  $\mathbf{S}$  to EVRP-TW-SPD is represented by a set of vehicle routes,  $\mathbf{S} = \{\mathbf{R}_1, \mathbf{R}_2, \dots, \mathbf{R}_K\}$ , where  $K$  is the number of vehicles used. Each route  $\mathbf{R}_i$  consists of a sequence of nodes that the EV visits,  $\mathbf{R}_i = (n_{i,1}, n_{i,2}, \dots, n_{i,L_i})$ , where  $n_{i,j}$  is the  $j$ -th node visited in  $\mathbf{R}_i$ , and  $L_i$  is the length of  $\mathbf{R}_i$ . For brevity, we temporarily omit the subscript  $i$  in  $\mathbf{R}_i$  in the following, i.e.,  $\mathbf{R} = (n_1, n_2, \dots, n_L)$ . The total travel distance of  $\mathbf{R}$ , denoted as  $TD(\mathbf{R})$ , is:

$$TD(\mathbf{R}) = \sum_{j=1}^{L-1} d_{n_j n_{j+1}}. \quad (1)$$

The battery energy state of the EV on arrival at and departure from  $n_j$ , denoted as  $y_{n_j}$  and  $Y_{n_j}$ , respectively, can be computed recursively as follows:

$$y_{n_j} = Y_{n_{j-1}} - h \cdot d_{n_{j-1} n_j}, \quad j > 1, \\ Y_{n_j} = \begin{cases} Q, & j = 1, \\ y_{n_j}, & j > 1, n_j \notin \mathbf{F}, \\ y_{n_j} + q_{n_j}, & j > 1, n_j \in \mathbf{F}, \end{cases} \quad (2)$$

where  $q_{n_j}$  is the charge amount at charging station  $n_j \in \mathbf{F}$ . An EV departs from the depot with a full battery. The arrival

and departure time at  $n_j$ , denoted as  $a_{n_j}$  and  $b_{n_j}$ , respectively, can be computed recursively as follows:

$$a_{n_j} = b_{n_{j-1}} + t_{n_{j-1} n_j}, \quad j > 1, \\ b_{n_j} = \begin{cases} e_0, & j = 1, \\ \max\{a_{n_j}, e_{n_j}\} + s_{n_j}, & j > 1, n_j \notin \mathbf{F}, \\ a_{n_j} + g \cdot q_{n_j}, & j > 1, n_j \in \mathbf{F}. \end{cases} \quad (3)$$

The EV load on arrival at  $n_j$ , denoted as  $load_{n_j}$ , is:

$$load_{n_j} = \begin{cases} \sum_{j=1}^L u_{n_j}, & j = 1, \\ load_{n_{j-1}} - u_{n_{j-1}} + v_{n_{j-1}}, & j > 1. \end{cases} \quad (4)$$

The total cost of  $\mathbf{S}$ , denoted as  $TC(\mathbf{S})$ , consists of two parts: the dispatching cost,  $\mu_1 \cdot K$ , and the transportation cost, which is the total travel distance of  $\mathbf{S}$  multiplied by the cost per unit of travel distance  $\mu_2$ . The objective is to find a solution with the minimum  $TC$ , as presented in Eq. (5a):

$$\min_{\mathbf{S}} TC(\mathbf{S}) = \mu_1 \cdot K + \mu_2 \cdot \sum_{i=1}^K TD(\mathbf{R}_i) \quad (5a)$$

$$\text{s.t. } n_{i,1} = n_{i,L_i} = 0, \quad 1 \leq i \leq K, \quad (5b)$$

$$\sum_{i=1}^K \sum_{j=2}^{L_i-1} \mathbb{I}[n_{i,j} = z] = 1, \quad 1 \leq z \leq M, \quad (5c)$$

$$0 \leq load_{n_{i,j}} \leq C, \quad 1 \leq i \leq K, \quad 1 \leq j \leq L_i, \quad (5d)$$

$$a_{n_{i,j}} \leq l_{n_{i,j}}, \quad 1 \leq i \leq K, \quad 2 \leq j \leq L_i, \quad (5e)$$

$$b_{n_{i,1}} \geq e_0 \text{ and } a_{n_{i,L_i}} \leq l_0, \quad 1 \leq i \leq K, \quad (5f)$$

$$0 \leq y_{n_{i,j}} \leq Y_{n_{i,j}} \leq Q, \quad 1 \leq i \leq K, \quad 1 \leq j \leq L_i. \quad (5g)$$

Constraint (5b) ensures that each route starts from and returns to the depot. Constraint (5c) ensures that each customer is served exactly once (note  $\mathbb{I}[\cdot]$  is the indicator function). Constraint (5d) ensures that the delivery and pickup demands of customers are met simultaneously while EVs do not exceed their loading capacity  $C$ . Constraint (5e) requires EVs to visit each node within its corresponding time window. Constraint (5f) ensures that EVs depart only after the start of the depot's time window and return before the end of its time window. Finally, constraint (5g) requires EVs to maintain a non-negative battery state at all nodes; when serving customers or visiting charging stations, the battery level will not decrease, and it will not exceed battery capacity  $Q$  when leaving any node.

In this work, unless otherwise specified, we evaluate solutions based on their cost (as their fitness) defined in Eq. (5a), where a lower cost indicates a better solution.

### IV. HYBRID MEMETIC ALGORITHM FOR EVRP-TW-SPD

In this section, we first introduce the two novel components integrated into HMA: PSSI for handling partial recharges and CDNS as the local search module. Then, we describe the overall framework of HMA.

---

**Algorithm 1:** PSSI

---

**Input:** an electricity-infeasible route:  $\mathbf{R}$   
**Output:** the best-found feasible route:  $\mathbf{R}^*$   
 /\* Parallel Station Insertion (PSI) \*/  
 1  $\bar{\mathbf{R}} \leftarrow$  remove all stations in  $\mathbf{R}$ ;  
 2  $\{(\mathbf{x}_1, \mathbf{R}_1), \dots, (\mathbf{x}_{\alpha L}, \mathbf{R}_{\alpha L})\} \leftarrow$  Initialization( $\bar{\mathbf{R}}, \alpha$ );  
 3 **while** max generation count  $B$  not reached **do**  
 4     **for**  $i \leftarrow 1$  to  $\alpha L$  **do**  
 5          $\mathbf{x}_{p_1}, \mathbf{x}_{p_2} \leftarrow$  Random\_Select( $\mathbf{x}_1, \mathbf{x}_2, \dots, \mathbf{x}_{\alpha L}$ );  
 6          $\mathbf{x}_{\text{child}} \leftarrow \mathbf{x}_{p_1} \oplus \mathbf{x}_{p_2}$ ;  
 7          $\mathbf{x}_{\text{child}} \leftarrow$  Mutation( $\mathbf{x}_{\text{child}}$ );  
 8          $\mathbf{R}_{\text{child}} \leftarrow$  insert stations into  $\bar{\mathbf{R}}$  according to  $\mathbf{x}_{\text{child}}$ ;  
 9         **if**  $\mathbf{R}_{\text{child}}$  is better than  $\mathbf{R}_i$  **then**  
 10              $(\mathbf{x}_i, \mathbf{R}_i) \leftarrow (\mathbf{x}_{\text{child}}, \mathbf{R}_{\text{child}})$ ;  
 11         **end**  
 12  $\mathbf{R}_{\text{PSI}} \leftarrow$  Select\_Best( $\mathbf{R}_1, \dots, \mathbf{R}_{\alpha L}$ );  
 /\* Sequential Station Insertion (SSI) \*/  
 13  $\mathbf{R}' \leftarrow \mathbf{R}$ ;  
 14 **while**  $\mathbf{R}'$  is electricity-infeasible **do**  
 15      $n_{\text{right}} \leftarrow$  the first node with negative battery state in  $\mathbf{R}'$ ;  
 16      $n_{\text{left}} \leftarrow$  the last station or depot visited before  $n_{\text{right}}$  in  $\mathbf{R}'$ ;  
 17      $\mathbf{R}' \leftarrow$  perform the best-possible station insertion in the path from  $n_{\text{left}}$  to  $n_{\text{right}}$ ;  
 18 **end**  
 19  $\mathbf{R}_{\text{SSI}} \leftarrow$  improve consecutive stations in  $\mathbf{R}'$ ;  
 20  $\mathbf{R}^* \leftarrow$  Select\_Best( $\mathbf{R}_{\text{PSI}}, \mathbf{R}_{\text{SSI}}$ );  
 21 **return**  $\mathbf{R}^*$

---

A. Parallel-Sequential Station Insertion (PSSI)

To transform electricity-infeasible routes into high-quality feasible routes, we propose a parallel-sequential station insertion (PSSI) procedure. Compared to existing sequential insertion procedures [15], [21], [22] that typically lead to sub-optimal routes, PSSI can better avoid local optima and generate higher-quality routes with acceptable additional computational cost. As shown in Algorithm 1, PSSI leverages two distinct strategies: parallel station insertion (PSI) and sequential station insertion (SSI). PSI (lines 1-12) employs a genetic algorithm to search for optimal station insertions between all consecutive customer pairs simultaneously, determining both the necessity of insertions and the inserted stations. SSI (lines 13-19), on the other hand, inserts charging stations sequentially along the route. Finally, PSSI selects the better route between PSI and SSI as the final outcome (line 20). By combining PSI and SSI, PSSI enables a more comprehensive exploration of the route space, potentially yielding higher-quality routes compared to purely sequential procedures.

As aforementioned in Section II, handling partial recharges involves two key aspects: station selection and charge amount calculation. In terms of station selection, PSI is designed for scenarios where at most one charging station is needed between any two consecutive nodes, while SSI allows multiple charging stations to be inserted between two consecutive nodes. Regarding charge amount calculation, both PSI and SSI use the same method. Below, we detail PSI and SSI based on these two aspects.

1) *Station Selection:* For a given problem instance  $\mathbf{G} = (\mathbf{V}', \mathbf{E})$ , we preprocess the charging stations to rank them for insertion between each pair of nodes. The ranking metric

is the extra cost induced by insertion, formally defined as  $d_{ik} + d_{kj} - d_{ij}$ , where  $k$  is a potential charging station to be inserted between nodes  $i$  and  $j$ . To balance efficiency and solution quality, only the top  $sr \cdot |\mathbf{F}|$  ranked charging stations are considered for insertion in both PSI and SSI, where  $sr \in (0, 1]$  is the selection range parameter.

PSI utilizes a genetic algorithm that consists of two main stages: initialization (lines 1-2) and evolution (lines 3-12). In the initialization stage, all charging stations are first removed from the input electricity-infeasible route  $\mathbf{R}$ , resulting in a fixed route  $\bar{\mathbf{R}} = (c_0, c_1, c_2, \dots, c_{L-1}, c_L)$ , where  $c_0 = c_L = 0$  represent the depot, and  $c_1, c_2, \dots, c_{L-1}$  are the  $L - 1$  customers. We define a binary decision variable  $X_{j,j+1}$  to indicate whether a charging station is inserted between  $c_j$  and  $c_{j+1}$  (1 for insertion, 0 for no insertion). Thus, the station insertion information is represented as a binary sequence  $\mathbf{x} = (X_{0,1}, X_{1,2}, \dots, X_{L-1,L})$ . An initial population of  $\alpha L$  binary sequences (i.e., the population size is proportional to  $L$ , with  $\alpha$  representing the proportionality parameter) is first generated, where each  $X_{j,j+1}$  is randomly set to 1 or 0 with equal probability (line 2). For each sequence, the binary encoding determines whether to insert a station between two consecutive nodes, and we always attempt to insert the highest-ranked station when insertion is indicated. If this insertion violates constraints, we try the next highest-ranked station until a feasible insertion is found or all stations within the selection range have been attempted. This process results in a set of feasible routes  $\mathbf{R}_1, \mathbf{R}_2, \dots, \mathbf{R}_{\alpha L}$ .

In the evolution stage, the population evolves over  $B$  generations. In each generation, two parent sequences are first randomly selected. A child sequence  $\mathbf{x}_{\text{child}}$  is generated using bitwise XOR crossover (denoted by  $\oplus$ ), inheriting unique insertion positions from each parent. Then, mutation is applied to  $\mathbf{x}_{\text{child}}$ : each bit has a low chance of flipping (i.e., 2%), followed by a high chance of flipping from 1 to 0 (i.e., 20%) to encourage fewer station insertions. The corresponding route  $\mathbf{R}_{\text{child}}$  is evaluated. Finally, a sequence in the population is replaced with  $\mathbf{x}_{\text{child}}$  if  $\mathbf{R}_{\text{child}}$  is with higher quality (line 9). The best route  $\mathbf{R}_{\text{PSI}}$  among the final population is selected as the outcome of PSI (line 12).

Unlike PSI, SSI progressively inserts stations along the route (lines 14-18). Specifically, for the first node  $n_{\text{right}}$  in the route with a negative battery level, it first finds the last charging station or depot visited before this node, denoted as  $n_{\text{left}}$ . Then, it evaluates all potential station insertions in the path from  $n_{\text{left}}$  to  $n_{\text{right}}$ . Finally, SSI selects the best feasible insertion to perform, i.e., the one that increases the route distance the least (lines 15-17). However, this greedy procedure can be short-sighted, particularly when multiple stations are inserted between two consecutive nodes. To address this limitation, the SSI procedure includes an additional refinement step (line 19). That is, for consecutive stations in the route, we attempt to replace them with stations based on the preprocessed rankings, starting from the highest-ranked to lower-ranked stations. If an improvement is found, the replacement is made. The final outcome of the SSI procedure is  $\mathbf{R}_{\text{SSI}}$ .

2) *Charge Amount Calculation:* We propose a new procedure tailored to EVRP-TW-SPD for calculating the partial

recharge amount, building upon the work of [16], [20]. Our approach considers both the minimal charge amount required and the available slack time, ensuring that the battery state is sufficient to reach the next charging station or depot while satisfying all time window constraints.

We define a path  $P_i = (f_i, c_{i,1}, c_{i,2}, \dots, c_{i,m_i}, f_{i+1})$  in route  $R$ , where  $f_i$  and  $f_{i+1}$  are two successive charging stations (or the depot) in the route, separated by  $m_i$  customers  $c_{i,j}$  ( $j = 1, \dots, m_i$ ). Our approach aims to minimize waiting time by utilizing any available slack time for additional charging. The charge amount at  $f_i$  consists of two parts: the minimal charge  $q_{f_i,0}$  and the additional charge  $q_{f_i,1}$ . Specifically,  $q_{f_i,0}$  is calculated as:

$$q_{f_i,0} = \max \left\{ 0, h \cdot TD(P_i) - y_{f_i} \right\}, \quad (6)$$

where  $h$  is the energy consumption rate and  $TD(P_i)$  is the total distance of path  $P_i$ .

To compute the additional charge  $q_{f_i,1}$ , we define the following variables. Let  $a'_{c_{i,j}}$ ,  $b'_{c_{i,j}}$  be the updated arrival and departure time at  $c_{i,j}$  (distinguished from  $a_{c_{i,j}}$ ,  $b_{c_{i,j}}$  in Section III),  $\delta_{i,j}$  be the slack time that can be used to charge due to waiting before starting service at  $c_{i,j}$ ,  $\tau_{i,j}$  be the potential available time that can be used to charge when leaving  $c_{i,j}$  while satisfying all previous time window constraints. Without loss of generality,  $f_i$  is regarded as  $c_{i,0}$  for notation convenience. Hence,  $q_{f_i,1}$  can be computed as:

$$q_{f_i,1} = \frac{1}{g} \sum_{j=1}^{m_i} \delta_{i,j}, \quad (7)$$

where  $g$  is the charging rate and  $\delta_{i,j}$  can be computed recursively as follows:

$$\begin{aligned} a'_{c_{i,j}} &= b'_{c_{i,j-1}} + t_{c_{i,j-1}c_{i,j}}, \quad j > 0, \\ b'_{c_{i,j}} &= \begin{cases} a_{f_i} + g \cdot q_{f_i,0}, & j = 0, \\ \max\{e_{c_{i,j}}, a'_{c_{i,j}} + \delta_{i,j}\} + s_{c_{i,j}}, & j > 0, \end{cases} \\ \delta_{i,j} &= \min\{\tau_{i,j-1}, \max\{0, e_{c_{i,j}} - a'_{c_{i,j}}\}\}, \quad j > 0, \\ \tau_{i,j} &= \begin{cases} \infty, & j = 0, \\ \min\{\tau_{i,j-1}, l_{c_{i,j}} - a'_{c_{i,j}}\} - \delta_{i,j}, & j > 0. \end{cases} \end{aligned} \quad (8)$$

When  $\tau_{i,j}$  is 0, the recursive equations can terminate prematurely. Upon reaching  $c_{i,m_i}$  of  $P_i$ , if no slack time is available, even if  $\tau_{i,m_i} > 0$ , no more charge time is needed. Thus, the additional charge  $q_{f_i,1}$  does not affect the arrival time at the next station  $f_{i+1}$ .

Finally, the total charge amount  $q_{f_i}$  that does not exceed  $Q - y_{f_i}$  when visiting  $f_i$  is computed as:

$$q_{f_i} = \min\{q_{f_i,0} + q_{f_i,1}, Q - y_{f_i}\}. \quad (9)$$

3) *Discussion*: Compared to existing purely sequential insertion procedures [15], [21], [22], PSSI can typically obtain higher-quality feasible routes with reasonable additional computational cost, as demonstrated in the experiments (see Section V-D). The applicability of PSSI extends beyond EVRP-TW-SPD to various EVRP variants sharing certain features: i) partial recharges, ii) customers with time windows, and iii)

---

**Algorithm 2: CDNS**


---

**Input:** a feasible solution:  $S$   
**Output:** a local optimum:  $S$   
 /\* Aggressive Local Search (ALS) \*/  
 1  $S' \leftarrow S$ ;  
 2  $\bar{S} \leftarrow$  remove all stations in  $S'$ ;  
 3 **repeat**  
 4      $\bar{S} \leftarrow$  apply an existing local search procedure for  
       VRP-TW-SPD to find the best-improving solution in  
       the neighborhood of  $\bar{S}$ ;  
 5     **for** each route  $R \in \bar{S}$  **do**  
 6          $R \leftarrow$  PSSI( $\bar{R}$ );  
 7         replace the corresponding route in  $S'$  with  $R$ ;  
 8     **end**  
 9     **if**  $S'$  is better than  $S$  **then**  $S \leftarrow S'$ ;  
 10 **until**  $\bar{S}$  is not improved or  $S'$  is electricity-infeasible;  
 /\* Conservative Local Search (CLS) \*/  
 11 **repeat**  
 12      $S \leftarrow$  find the best-improving solution in the  
       EVRP-TW-SPD neighborhood of  $S$ ;  
 13 **until**  $S$  is not improved;  
 14 **return**  $S$

---

a homogeneous network of charging stations. For instance, PSSI could be applied to scenarios involving multiple depots, heterogeneous vehicle fleets, or even dynamic routing where customer demands or traffic conditions change in real-time.

### B. Cross-Domain Neighborhood Search (CDNS)

We propose cross-domain neighborhood search (CDNS), a novel local search procedure that explores two distinct solution spaces simultaneously: the solution space of EVRP-TW-SPD and the solution space of its non-electric counterpart VRP-TW-SPD [19], where some solutions may be infeasible for EVRP-TW-SPD. This cross-domain exploration offers two key advantages. First, by expanding beyond the feasible solution space of EVRP-TW-SPD, CDNS potentially discovers higher-quality solutions that might be overlooked by conventional single-domain local search. Second, exploring the solution space of VRP-TW-SPD enables the efficient reuse of well-established local search procedures for VRP-TW-SPD. We will further discuss the broader implications of this cross-domain approach beyond EVRP-TW-SPD at the end of Section IV-B.

The core idea of CDNS is to exploit the relationship between feasible solutions of EVRP-TW-SPD and VRP-TW-SPD [19], as stated below.

**Proposition 1.** Given an EVRP-TW-SPD instance, removing all charging stations from a feasible EVRP-TW-SPD solution always results in a feasible VRP-TW-SPD solution.

The proof can be found in Appendix A. Conversely, to transform a feasible VRP-TW-SPD solution to a feasible EVRP-TW-SPD solution, we can use the aforementioned PSSI procedure.

Algorithm 2 outlines the framework of CDNS. It consists of two sub-procedures. The first, called aggressive local search (ALS), explores the solution space of VRP-TW-SPD. As its name suggests, it temporarily ignores the electricity constraint (5g) and repeatedly applies existing local search

procedures for VRP-TW-SPD to find the solution with maximum improvement (i.e., the best-improving solution) in the neighborhood of the current solution (lines 1-10). When ALS can no longer improve the solution, CDNS switches to conservative local search (CLS) which searches for improvements within the solution space of EVRP-TW-SPD (lines 11-13). Below we detail these two sub-procedures.

1) *Aggressive Local Search (ALS)*: When a feasible solution  $S$  to EVRP-TW-SPD enters ALS (lines 1-10), the first step is to remove all charging stations in  $S$ , resulting in a feasible solution  $\bar{S}$  to VRP-TW-SPD (line 2). Then, an existing local search procedure for VRP-TW-SPD is repeatedly applied to find the best-improving solution in the neighborhood of  $\bar{S}$  (line 4). Here, we employ the local search procedure of MATE [19], one of the state-of-the-art algorithms for solving VRP-TW-SPD. This procedure involves multiple move operators and constant-time move evaluation (see the paper of MATE for details). Then, for each found best-improving solution, PSSI is first applied to transform it into a feasible EVRP-TW-SPD solution (lines 5-8). If this transformation is not possible, then ALS would terminate (i.e., the second termination condition in line 10). If successful, the resulting feasible solution would replace the current solution  $S$  when it has better quality (line 9). ALS would terminate when no further improvement is possible (i.e., the first termination condition in line 10).

2) *Conservative Local Search (CLS)*: Unlike ALS, CLS performs local search directly in the solution space of EVRP-TW-SPD. It repeatedly identifies the best-improving solution in the current solution's neighborhood until no further improvement is possible (lines 11-13). The neighborhood is defined by the following five move operators.

- *2-opt*: it inverts a subsequence of two consecutive customers in a route.
- *2-opt\**: it removes two arcs from two different routes, splitting each into two parts, then reconnects the first part of one route with the second part of the other, and vice versa.
- *or-opt*: it removes one or two consecutive customers from a route and reinserts them elsewhere in the same or a different route.
- *swap*: it exchanges two non-overlapping subsequences of one or two consecutive customers, either within the same route or across different routes.
- *relocate*: it moves a customer from its current position to a new position, either within the same route or to a different route.

3) *Discussion*: By exploring two distinct solution spaces, CDNS typically finds higher-quality solutions than using either solution space alone, as demonstrated in our experiments (see Section V-D). The idea of CDNS can be readily generalized to other EVRP variants by simultaneously exploring both electric and non-electric neighborhoods. This dual-domain approach is particularly valuable since non-electric variants are typically more extensively studied in the literature, providing a rich pool of well-established local search procedures that can be adapted for solving various EVRPs efficiently.

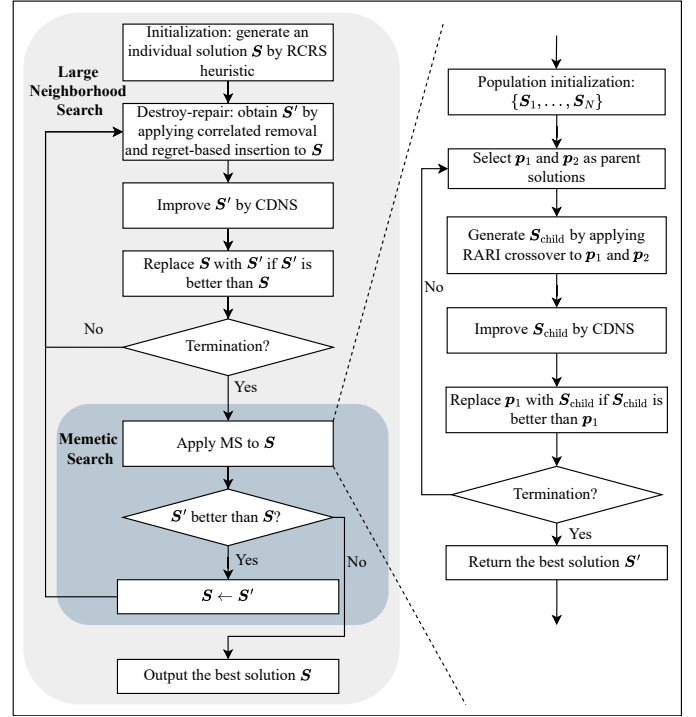


Fig. 1. The flow chart of HMA.

### C. Overall Framework of HMA

We now introduce the framework of HMA, which integrates an individual-based large neighborhood search (LNS) and a population-based memetic search (MS). The flow chart of HMA is illustrated in Figure 1. Overall, HMA employs LNS to efficiently obtain a high-quality solution, and then uses MS to further improve it.

As presented in Algorithm 3, HMA first enters the individual-based LNS. It begins with the initialization of an individual solution  $S$ , which is constructed using the RCRS heuristic [13]. Specifically, RCRS is an extension of the cheapest-insertion heuristic and constructs routes by iteratively inserting an unassigned customer at the position with the minimal value according to the RCRS criterion until no feasible insertions are possible due to capacity or time window constraints (please refer to [13] for details of RCRS). The RCRS criterion combines the total travel distance, residual capacity, and radial surcharge with weighting parameters  $\lambda, \gamma \in [0, 1]$ . Here, we simply set  $\lambda = \gamma = 0.5$ . In this initialization, electricity-feasible customers are first considered for insertion, followed by those that are only electricity-infeasible but can be handled later through best station insertion. When no feasible insertions remain, a new route is initiated. This process continues until all customers are assigned (line 1).

After initialization, HMA applies the destroy-repair operator as described in [19] (a large-step perturbation) on the individual solution  $S$  (line 4). This destroy-repair operator involves removing  $\rho$  correlated customers from the solution, where the random number  $\rho \in [\omega_1|V|, \omega_2|V|]$ , and  $\omega_1, \omega_2$  are parameters with  $0 < \omega_1 \leq \omega_2 < 1$ . The operator then reinserts these customers using a regret-based heuristic that

**Algorithm 3: HMA**


---

**Input:** an EVRP-TW-SPD instance:  $G = (V', E)$   
**Output:** the best-found solution:  $S$

```

/* Large Neighborhood Search (LNS) */
1 {S} ← Initialization();
2 while true do
3   S' ← S;
4   remove ρ customers from S' and reinsert them into S'
   via regret-based insertion;
5   S' ← CDNS(S');
6   if S' is better than S then S ← S';
7   if S is not improved in the last G iterations then
   /* Memetic Search (MS) */
8     S' ← S;
9     {S1, ..., SN} ← Population_Initialization(S');
10    repeat
11      π(·) ← a random permutation of 1, ..., N;
12      for i ← 1 to N do
13        p1 ← Sπ(i), p2 ← Sπ(i+1);
14        Schild ← Crossover(p1, p2);
15        Schild ← CDNS(Schild);
16        Sπ(i) ← Select_Best(Schild, p1);
17      end
18      S' ← Select_Best(S', S1, ..., SN);
19    until S' is not improved in the last G generations;
20    if S' is better than S then S ← S';
21    else break;
22  end
23 end
24 return S

```

---

evaluates the expected cost of inserting a node in a future iteration rather than in the current one to assess the quality of potential insertions. The process is followed by CDNS, ensuring that a new local optimum is reached to potentially improve  $S$  (lines 5-6). If  $S$  does not show improvement over a specified number of consecutive iterations, denoted as  $G$ , HMA initiates the population-based MS (lines 8-19).

MS starts with a population of  $N$  individuals  $S_1, \dots, S_N$ , generated based on the current elite solution  $S$  (line 9). Specifically,  $S_1$  is set as a copy of  $S$  because the elite solution should be preserved. As for the remaining individuals, the individual  $S_i$  with odd index  $i$  comes from the destroy-repair operator performed on  $S$  with  $\omega_1 = \omega_2 = i/N$ ; for the individual  $S_i$  with even index  $i$ , it is generated by RCRS with  $\lambda = \frac{1}{\sqrt{N-1}} \cdot (p-1)$ ,  $\gamma = \frac{1}{\sqrt{N-1}} \cdot (q-1)$ , where  $p = \lceil i/\sqrt{N} \rceil$  and  $q = i - \sqrt{N} \cdot (p-1)$ . The above procedure would result in a diverse population of individuals while preserving the high-quality information of the elite solution obtained from the previous LNS.

After initialization, MS enters an evolutionary process (lines 10-19). In each generation (lines 12-17), each individual in the population is selected once as parent  $p_1$  and once as parent  $p_2$ , in a random order (lines 11 and 13). For each pair of parent solutions, MS generates an offspring using the route-assembly-regret-insertion (RARI) crossover [19] (line 14), and then improves it through CDNS (line 15). After that, the better one among the offspring and  $p_1$  replaces the individual selected as  $p_1$  (line 16). After MS, a new candidate solution  $S'$  is obtained with the aim of improving  $S$  (lines 20-21). If

TABLE I  
SETTING OF ALGORITHM PARAMETERS.

| Parameter      | $G$ | $N$ | $\alpha$ | $B$ | $sr$ | $w_1, w_2$ |
|----------------|-----|-----|----------|-----|------|------------|
| $akb_{small}$  | 20  | 9   | 3        | 5   | 1.0  | 0.2, 0.4   |
| $akb_{medium}$ | 20  | 4   | 3        | 5   | 0.5  | 0.1, 0.2   |
| $jd$           | 20  | 4   | 3        | 5   | 0.1  | 0.05, 0.05 |

the quality of  $S$  is still not improved by MS, then HMA would output  $S$  and terminate (line 21); otherwise, HMA proceeds to the next iteration of LNS (line 20).

When presented with a large-scale problem instance (with more than 200 customers) to solve, we make two adjustments to HMA to improve its efficiency. First, only ALS is used in CDNS. Second, problem decomposition is employed in MS. Specifically, the decomposition breaks down the main problem  $G = (V', E)$  into  $k$  smaller subproblems  $G_1, \dots, G_k$  when entering MS (line 8). A subproblem  $G_i = (V'_i, E_i)$  with  $V'_i = \{0\} \cup V_i \cup F$ ,  $E_i = \{(p, q) | p, q \in V'_i, p \neq q\}$ , where  $V = \bigcup_{i=1}^k V_i$  and  $V_i \cap V_j = \emptyset \forall i \neq j$ ,  $1 \leq i, j \leq k$ . Here, we use the barycenter clustering decomposition (BCD) [33] to determine the partition of  $V_i$ . The barycenter of a route  $R = (n_1, n_2, \dots, n_L)$  is defined as  $(\bar{x}, \bar{y}) = \frac{1}{L-1} \sum_{i=1}^{L-1} (x_i, y_i)$ , where  $(x_i, y_i)$  is the Cartesian plane coordinate of node  $n_i$ . For each subproblem  $G_i$ , the same MS is applied (lines 9-19). After all MS procedures are finished, the solutions from all subproblems are assembled to construct a complete solution  $S'$  for the original problem.

## V. EXPERIMENTS

To evaluate the effectiveness of HMA, we compared it with the recent algorithms for solving EVRP-TW-SPD, Adapt-CMSA-STD [11] and Adapt-CMSA-SETCOV [17], using the existing benchmark set. Then, we introduced a new benchmark set derived from a real-world application that includes large-scale instances. The evaluation results of HMA on the new benchmark were also reported. Finally, we conducted a comprehensive ablation study to assess the effectiveness of PSSI, CDNS, and the hybrid search framework. The source code of HMA and the new benchmark set are open-sourced anonymously at <https://anonymous.4open.science/r/EVRP-TW-SPD-HMA-code-dataset>.

### A. Experimental Setup

1) *Benchmark:* As noted by Akbay *et al.* [11], the existing benchmark used is based on E-VRPTW instances from Schneider *et al.* [12], with customer demands separated into delivery and pickup demands using the method in [34]. We refer to this benchmark as the *akb* (authors' initials) set. This *akb* set has 92 instances, including 36 small-scale instances (twelve 5-customer instances, twelve 10-customer instances, and twelve 15-customer instances, each with 2 to 8 stations) and 56 medium-scale instances (100-customer instances with 21 stations). These instances are categorized into three groups based on the spatial distribution of customer locations: clustered

TABLE II  
COMPARATIVE RESULTS ON SMALL-SCALE INSTANCES IN THE *akb* SET.

| Instance | CPLEX |         |          | Adapt-CMSA-STD |         |         |       | Adapt-CMSA-SETCOV |         |         |       | HMA  |         |         |       |
|----------|-------|---------|----------|----------------|---------|---------|-------|-------------------|---------|---------|-------|------|---------|---------|-------|
|          | m     | best    | time     | m              | best    | avg     | time  | m                 | best    | avg     | time  | m    | best    | avg     | time  |
| c101C5   | 2     | 2257.75 | 0.43     | 2              | 2257.75 | 2257.75 | 0.02  | 2                 | 2257.75 | 2257.75 | 0.01  | 2    | 2257.75 | 2257.75 | 0.38  |
| c103C5   | 1     | 1175.37 | 0.41     | 1              | 1175.37 | 1175.37 | 0.54  | 1                 | 1175.37 | 1175.37 | 0.68  | 1    | 1175.37 | 1175.37 | 0.21  |
| c206C5   | 1     | 1242.56 | 0.58     | 1              | 1242.56 | 1242.56 | 0.03  | 1                 | 1242.56 | 1242.56 | 0.00  | 1    | 1242.56 | 1242.56 | 0.19  |
| c208C5   | 1     | 1158.48 | 0.08     | 1              | 1158.48 | 1158.48 | 0.01  | 1                 | 1158.48 | 1158.48 | 0.00  | 1    | 1158.48 | 1158.48 | 0.24  |
| r104C5   | 2     | 2136.69 | 0.02     | 2              | 2136.69 | 2136.69 | 0.07  | 2                 | 2136.69 | 2136.69 | 0.01  | 2    | 2136.69 | 2136.69 | 0.93  |
| r105C5   | 2     | 2156.08 | 0.03     | 2              | 2156.08 | 2156.08 | 0.01  | 2                 | 2156.08 | 2156.08 | 0.00  | 2    | 2156.08 | 2156.08 | 1.28  |
| r202C5   | 1     | 1128.78 | 0.06     | 1              | 1128.78 | 1128.78 | 9.00  | 1                 | 1128.78 | 1128.78 | 0.00  | 1    | 1128.78 | 1128.78 | 0.24  |
| r203C5   | 1     | 1179.06 | 0.03     | 1              | 1179.06 | 1179.06 | 0.22  | 1                 | 1179.06 | 1179.06 | 0.05  | 1    | 1179.06 | 1179.06 | 0.17  |
| rc105C5  | 2     | 2233.77 | 2.18     | 2              | 2233.77 | 2233.77 | 0.09  | 2                 | 2233.77 | 2233.77 | 0.04  | 2    | 2233.77 | 2233.77 | 0.86  |
| rc108C5  | 2     | 2253.93 | 0.19     | 2              | 2253.93 | 2253.93 | 0.01  | 2                 | 2253.93 | 2253.93 | 0.00  | 2    | 2253.93 | 2253.93 | 0.58  |
| rc204C5  | 1     | 1176.39 | 0.25     | 1              | 1176.39 | 1176.39 | 0.07  | 1                 | 1176.39 | 1176.39 | 0.01  | 1    | 1176.39 | 1176.39 | 0.21  |
| rc208C5  | 1     | 1167.98 | 0.12     | 1              | 1167.98 | 1167.98 | 0.52  | 1                 | 1167.98 | 1167.98 | 0.03  | 1    | 1167.98 | 1167.98 | 0.19  |
| c101C10  | 3     | 3388.25 | 76.74    | 3              | 3388.25 | 3388.25 | 0.28  | 3                 | 3388.25 | 3388.55 | 0.33  | 3    | 3388.25 | 3388.25 | 1.70  |
| c104C10  | 2     | 2273.93 | 2.16     | 2              | 2273.93 | 2273.93 | 0.48  | 2                 | 2273.93 | 2273.93 | 29.02 | 2    | 2273.93 | 2273.93 | 1.10  |
| c202C10  | 1     | 1304.06 | 6.34     | 1              | 1304.06 | 1304.06 | 0.45  | 1                 | 1304.06 | 1304.06 | 0.10  | 1    | 1304.06 | 1304.06 | 1.40  |
| c205C10  | 2     | 2228.28 | 0.08     | 2              | 2228.28 | 2228.28 | 10.82 | 2                 | 2228.28 | 2228.28 | 0.03  | 2    | 2228.28 | 2228.28 | 0.45  |
| r102C10  | 3     | 3249.19 | 0.56     | 3              | 3249.19 | 3249.19 | 18.22 | 3                 | 3249.19 | 3249.19 | 0.01  | 3    | 3249.19 | 3249.19 | 1.03  |
| r103C10  | 2     | 2206.12 | 17.49    | 2              | 2206.12 | 2206.12 | 5.27  | 2                 | 2206.12 | 2206.12 | 22.01 | 2    | 2206.12 | 2206.12 | 3.38  |
| r201C10  | 1     | 1241.51 | 61.20    | 1              | 1241.51 | 1241.51 | 22.71 | 1                 | 1241.51 | 1241.51 | 15.97 | 1    | 1241.51 | 1241.51 | 3.29  |
| r203C10  | 1     | 1218.21 | 1.57     | 1              | 1218.21 | 1218.21 | 14.06 | 1                 | 1218.21 | 1218.21 | 27.17 | 1    | 1218.21 | 1218.21 | 0.97  |
| rc102C10 | 4     | 4423.51 | 0.15     | 4              | 4423.51 | 4423.51 | 0.24  | 4                 | 4423.51 | 4423.51 | 0.01  | 4    | 4423.51 | 4423.51 | 3.27  |
| rc108C10 | 3     | 3345.93 | 3.72     | 3              | 3345.93 | 3345.93 | 14.61 | 3                 | 3345.93 | 3345.93 | 0.01  | 3    | 3345.93 | 3345.93 | 1.29  |
| rc201C10 | 1     | 1412.86 | 22756.49 | 1              | 1412.86 | 1412.86 | 1.97  | 1                 | 1412.86 | 1412.86 | 0.93  | 1    | 1412.86 | 1412.86 | 6.03  |
| rc205C10 | 2     | 2325.98 | 0.13     | 2              | 2325.98 | 2325.98 | 0.13  | 2                 | 2325.98 | 2325.98 | 0.45  | 2    | 2325.98 | 2325.98 | 0.74  |
| c103C15  | 3     | 3348.46 | 5046.46  | 3              | 3348.46 | 3348.47 | 48.19 | 3                 | 3348.46 | 3348.46 | 3.76  | 3    | 3348.46 | 3348.46 | 3.30  |
| c106C15  | 3     | 3275.13 | 0.90     | 3              | 3275.13 | 3275.13 | 4.56  | 3                 | 3275.13 | 3275.13 | 32.34 | 3    | 3275.13 | 3275.13 | 2.42  |
| c202C15  | 2     | 2383.62 | 43.74    | 2              | 2383.62 | 2383.62 | 12.73 | 2                 | 2383.62 | 2393.39 | 5.27  | 2    | 2383.62 | 2383.62 | 1.67  |
| c208C15  | 2     | 2300.55 | 3.25     | 2              | 2300.55 | 2300.55 | 1.09  | 2                 | 2300.55 | 2300.55 | 8.59  | 2    | 2300.55 | 2300.55 | 1.36  |
| r102C15  | 5     | 5412.78 | 5046.62  | 5              | 5412.78 | 5412.78 | 1.82  | 5                 | 5412.78 | 5412.78 | 0.09  | 5    | 5412.78 | 5412.78 | 4.27  |
| r105C15  | 4     | 4336.15 | 5.34     | 4              | 4336.15 | 4336.15 | 1.03  | 4                 | 4336.15 | 4336.15 | 0.86  | 4    | 4336.15 | 4336.15 | 2.03  |
| r202C15  | 2     | 2361.51 | 5045.36  | 2              | 2358.00 | 2364.90 | 22.71 | 1                 | 1507.32 | 1677.46 | 45.16 | 2    | 2358.00 | 2358.00 | 4.00  |
| r209C15  | 1     | 1313.24 | 3088.27  | 1              | 1313.24 | 1313.24 | 12.23 | 1                 | 1313.24 | 1313.24 | 10.98 | 1    | 1313.24 | 1313.24 | 2.83  |
| rc103C15 | 4     | 4397.67 | 245.61   | 4              | 4397.67 | 4397.67 | 0.24  | 4                 | 4397.67 | 4397.67 | 0.21  | 4    | 4397.67 | 4397.67 | 2.73  |
| rc108C15 | 3     | 3370.25 | 822.47   | 3              | 3370.25 | 3370.25 | 41.34 | 3                 | 3370.25 | 3370.25 | 0.24  | 3    | 3370.25 | 3370.25 | 1.87  |
| rc202C15 | 2     | 2394.39 | 603.76   | 2              | 2394.39 | 2394.39 | 0.48  | 2                 | 2394.39 | 2394.39 | 19.65 | 2    | 2394.39 | 2394.39 | 2.72  |
| rc204C15 | 1     | 1403.38 | 5046.60  | 1              | 1382.22 | 1385.72 | 47.83 | 1                 | 1382.22 | 1382.55 | 50.49 | 1    | 1382.22 | 1384.83 | 19.75 |
| avg      | 2.06  | 2338.38 | 1331.37  | 2.06           | 2337.70 | 2337.99 | 8.17  | 2.03              | 2314.07 | 2319.08 | 7.62  | 2.06 | 2337.70 | 2337.77 | 2.20  |

(prefixed with *c*), randomly distributed (prefixed with *r*), and a mixture of random and clustered distributions (prefixed with *rc*). Each group is further divided into two sub-classes: type 1 features narrow time windows and small vehicle and battery capacities, while type 2 has wide time windows and large vehicle and battery capacities. All these instances are defined in a two-dimensional Euclidean space. That is, each node *i* has the Cartesian coordinate  $(x_i, y_i)$ . The distance between two nodes *i* and *j* is given by the Euclidean distance  $\sqrt{(x_i - x_j)^2 + (y_i - y_j)^2}$ , which is a special case of the problem formulation provided in this paper (see Section III). All distances and time between two nodes *i* and *j* satisfy the triangle inequality. Following [11], [17], in the experiments conducted on the *akb* set, we set  $\mu_1 = 1000$  and  $\mu_2 = 1$ .

As previously mentioned, the *akb* set includes only synthetic instances of small and medium scales. To address the gap in benchmark instance scales, we introduced a new benchmark set derived from JD Logistics' distribution system. The raw data collected from this system includes requests over a period in Beijing, involving both deliveries of purchased goods and collections picked up from customers. We sampled from this data to generate instances with 200, 400, 600, 800, and 1000 customers, each with 100 stations. For each problem scale, we generated 4 instances, resulting in a set of 20 large-scale instances, referred to as the *jd* set. Since the *jd* dataset is derived from real-world data, each instance provides the

longitude and latitude  $(lng_i, lat_i)$  of each node *i*, in degrees. Additionally, the distances and time between two nodes *i* and *j* might not satisfy the triangle inequality, which represents a general real-world case of the problem formulation. Unlike the *akb* set,  $\mu_1 = 300$  and  $\mu_2 = 0.014$  in the *jd* set are directly given based on the estimated values in the application.

2) *Parameter Setting*: We determined the parameter settings of HMA through preliminary experiments. The settings for different problem scales are detailed in Table I. Specifically, HMA requires setting six parameters: *G*, *N*,  $\alpha$ , *B*, *sr*, and  $w_1, w_2$ . *G* denotes the longest consecutive generation without improvement in HMA, and *N* is the population size in MS (see Algorithm 3).  $\alpha$  and *B* refer to the proportionality parameter and the maximum number of generations in PSI, respectively. *sr* specifies the selection range in station ranking list (see Algorithm 1).  $w_1$  and  $w_2$  are the lower and upper bounds for the proportion of customers removed in the destroy-repair operator (see Algorithm 3). All the experiments were run on an Intel Xeon Gold 6240 machine with 377 GB RAM and 32 cores (2.60 GHz, 25 MB Cache), running Rocky Linux 8.5. HMA was implemented in C++.

### B. Results on Small-scale and Medium-scale Instances

We compared HMA with two recently proposed algorithms, Adapt-CMSA-STD and Adapt-CMSA-SETCOV, on the *akb* set. Since their source code is not publicly available, we

TABLE III  
COMPARATIVE RESULTS ON MEDIUM-SCALE INSTANCES IN THE AKB SET.

| Instance | Adapt-CMSA-STD |          |          |        | Adapt-CMSA-SETCOV |          |          |        | HMA  |          |          |        |
|----------|----------------|----------|----------|--------|-------------------|----------|----------|--------|------|----------|----------|--------|
|          | m              | best     | avg      | time   | m                 | best     | avg      | time   | m    | best     | avg      | time   |
| c101     | 12             | 13043.40 | 13043.42 | 270.56 | 12                | 13057.80 | 13063.54 | 205.53 | 12   | 13043.38 | 13043.43 | 12.57  |
| c102     | 11             | 12056.80 | 12920.23 | 393.95 | 11                | 12073.10 | 12944.34 | 329.34 | 10   | 11089.80 | 12033.33 | 83.87  |
| c103     | 11             | 12004.70 | 12026.90 | 317.63 | 10                | 11134.90 | 11917.80 | 504.47 | 10   | 10945.45 | 10945.48 | 136.32 |
| c104     | 10             | 10872.80 | 11353.78 | 442.55 | 10                | 10870.70 | 10876.49 | 427.43 | 9    | 9890.98  | 10767.31 | 231.74 |
| c105     | 11             | 12023.80 | 12341.60 | 394.88 | 11                | 12034.10 | 12068.86 | 409.38 | 11   | 12030.81 | 12130.20 | 64.75  |
| c106     | 11             | 12013.10 | 12438.06 | 458.04 | 11                | 12025.70 | 12059.29 | 305.45 | 10   | 11040.32 | 11825.37 | 73.50  |
| c107     | 11             | 12006.40 | 12023.97 | 378.24 | 11                | 12026.70 | 12046.38 | 276.09 | 10   | 11021.16 | 11815.55 | 67.93  |
| c108     | 11             | 11994.70 | 12016.10 | 407.11 | 10                | 11025.80 | 11822.60 | 391.00 | 10   | 11006.10 | 11597.49 | 137.57 |
| c109     | 10             | 11042.20 | 11885.30 | 502.22 | 10                | 10941.00 | 11180.77 | 524.19 | 10   | 10911.47 | 10936.41 | 184.63 |
| c201     | 4              | 4629.95  | 4629.95  | 26.41  | 4                 | 4678.37  | 4703.43  | 274.65 | 4    | 4629.95  | 4629.95  | 9.55   |
| c202     | 4              | 4629.95  | 4629.95  | 192.19 | 4                 | 4664.26  | 4706.94  | 277.38 | 4    | 4629.95  | 4629.95  | 34.02  |
| c203     | 4              | 4632.27  | 4690.06  | 520.20 | 4                 | 4641.45  | 4734.31  | 349.57 | 4    | 4629.95  | 4629.95  | 47.47  |
| c204     | 4              | 4633.08  | 4665.78  | 563.25 | 4                 | 4660.64  | 4737.07  | 503.66 | 4    | 4628.91  | 4628.91  | 102.73 |
| c205     | 4              | 4629.95  | 4629.95  | 54.00  | 4                 | 4629.95  | 4629.95  | 88.12  | 4    | 4629.95  | 4629.95  | 31.58  |
| c206     | 4              | 4629.95  | 4629.95  | 149.83 | 4                 | 4629.95  | 4629.95  | 142.64 | 4    | 4629.95  | 4630.26  | 39.25  |
| c207     | 4              | 4629.95  | 4629.95  | 179.74 | 4                 | 4629.95  | 4635.27  | 182.89 | 4    | 4629.95  | 4630.89  | 62.34  |
| c208     | 4              | 4629.95  | 4629.95  | 200.06 | 4                 | 4629.95  | 4629.95  | 183.86 | 4    | 4629.95  | 4629.95  | 50.89  |
| r101     | 18             | 19633.80 | 19939.79 | 459.20 | 18                | 19640.60 | 19661.15 | 476.75 | 17   | 18636.96 | 19512.43 | 75.46  |
| r102     | 17             | 18470.80 | 19292.16 | 496.96 | 16                | 17474.10 | 17696.35 | 561.10 | 16   | 17424.75 | 17526.29 | 115.80 |
| r103     | 15             | 16296.50 | 17050.75 | 499.65 | 14                | 15280.30 | 15306.17 | 449.49 | 13   | 14209.21 | 14721.75 | 187.46 |
| r104     | 13             | 14141.10 | 14255.53 | 433.34 | 12                | 13084.30 | 13111.31 | 538.23 | 11   | 12051.19 | 12066.53 | 285.75 |
| r105     | 15             | 16389.20 | 17212.83 | 477.88 | 14                | 15471.30 | 16346.10 | 429.92 | 14   | 15366.33 | 16159.23 | 146.98 |
| r106     | 15             | 16292.00 | 16836.67 | 492.99 | 14                | 15314.80 | 15441.68 | 524.23 | 13   | 14265.55 | 14373.31 | 222.14 |
| r107     | 13             | 14168.90 | 15016.67 | 478.40 | 12                | 13140.10 | 13669.50 | 550.64 | 12   | 13112.66 | 13118.04 | 226.39 |
| r108     | 12             | 13079.80 | 13531.30 | 468.60 | 11                | 12073.70 | 12998.17 | 521.61 | 11   | 12016.74 | 12025.10 | 289.00 |
| r109     | 14             | 15237.30 | 15674.51 | 533.66 | 13                | 14220.80 | 14468.12 | 523.07 | 12   | 13203.74 | 13993.94 | 237.95 |
| r110     | 13             | 14170.20 | 14905.73 | 370.99 | 12                | 13114.30 | 13544.76 | 541.43 | 11   | 12070.04 | 12482.82 | 270.95 |
| r111     | 12             | 13144.20 | 14584.19 | 489.45 | 12                | 13148.80 | 13965.98 | 503.08 | 12   | 13070.64 | 13077.15 | 225.63 |
| r112     | 12             | 13155.60 | 14053.56 | 331.29 | 12                | 13044.10 | 13078.65 | 597.35 | 11   | 12001.79 | 12012.62 | 233.83 |
| r201     | 4              | 5192.33  | 5216.92  | 506.12 | 4                 | 5276.75  | 5363.04  | 131.64 | 3    | 4268.88  | 4985.55  | 264.02 |
| r202     | 3              | 4250.70  | 5020.88  | 483.79 | 3                 | 4193.33  | 4940.22  | 615.58 | 3    | 4054.75  | 4063.20  | 363.02 |
| r203     | 3              | 3942.74  | 4352.52  | 609.82 | 3                 | 3985.02  | 4060.18  | 577.82 | 3    | 3898.68  | 3910.77  | 541.38 |
| r204     | 3              | 3820.72  | 3854.31  | 553.01 | 3                 | 3793.76  | 3827.81  | 615.67 | 2    | 2815.58  | 3544.13  | 438.26 |
| r205     | 3              | 4055.28  | 4124.64  | 514.20 | 3                 | 4065.06  | 4126.45  | 253.23 | 3    | 3995.35  | 4003.09  | 512.99 |
| r206     | 3              | 3978.10  | 4065.05  | 531.38 | 3                 | 3991.44  | 4047.16  | 550.82 | 3    | 3925.95  | 3938.12  | 600.35 |
| r207     | 3              | 3878.91  | 3910.07  | 463.55 | 3                 | 3881.97  | 3918.29  | 616.95 | 2    | 2851.75  | 3534.37  | 494.20 |
| r208     | 3              | 3791.27  | 3829.39  | 596.95 | 3                 | 3732.80  | 3776.20  | 629.30 | 2    | 2740.06  | 2756.80  | 589.42 |
| r209     | 3              | 3975.64  | 4015.90  | 467.75 | 3                 | 3933.55  | 3977.24  | 538.01 | 3    | 3877.24  | 3885.71  | 636.14 |
| r210     | 3              | 3920.37  | 3984.78  | 530.97 | 3                 | 3926.79  | 3961.42  | 520.11 | 3    | 3846.62  | 3854.33  | 555.78 |
| r211     | 3              | 3814.42  | 3893.38  | 580.24 | 3                 | 3824.47  | 3857.62  | 561.62 | 3    | 3772.67  | 3789.62  | 477.61 |
| rc101    | 16             | 17667.70 | 18513.67 | 504.48 | 16                | 17696.20 | 17741.63 | 442.05 | 15   | 16661.53 | 17462.90 | 152.22 |
| rc102    | 16             | 17576.80 | 17909.78 | 392.20 | 15                | 16558.20 | 16628.46 | 422.70 | 14   | 15510.31 | 15618.29 | 256.61 |
| rc103    | 14             | 15366.90 | 16245.06 | 537.04 | 13                | 14358.20 | 14999.16 | 485.96 | 12   | 13343.56 | 13648.08 | 297.57 |
| rc104    | 13             | 14270.50 | 14315.17 | 447.54 | 12                | 13222.50 | 13261.65 | 490.66 | 11   | 12150.47 | 12168.35 | 388.45 |
| rc105    | 15             | 16500.90 | 16933.42 | 458.25 | 14                | 15470.70 | 15820.90 | 449.50 | 14   | 15447.52 | 15454.71 | 164.64 |
| rc106    | 14             | 15432.50 | 16069.05 | 444.10 | 13                | 14448.30 | 15249.17 | 406.17 | 13   | 14388.12 | 14609.85 | 190.86 |
| rc107    | 13             | 14313.40 | 14437.31 | 540.67 | 12                | 13276.50 | 13386.51 | 518.89 | 11   | 12234.76 | 13048.02 | 232.42 |
| rc108    | 12             | 13226.00 | 13891.71 | 435.95 | 12                | 13184.70 | 13214.50 | 504.05 | 11   | 12140.28 | 12152.42 | 271.54 |
| rc201    | 4              | 5504.77  | 5819.06  | 494.52 | 4                 | 5617.75  | 5786.48  | 226.81 | 4    | 5444.90  | 5450.77  | 254.36 |
| rc202    | 4              | 5324.64  | 5442.41  | 416.84 | 4                 | 5436.63  | 5541.80  | 138.34 | 4    | 5240.40  | 5249.87  | 192.66 |
| rc203    | 4              | 5109.88  | 5177.69  | 452.57 | 4                 | 5086.44  | 5159.15  | 531.94 | 3    | 4078.55  | 4100.32  | 597.82 |
| rc204    | 3              | 4036.49  | 4525.03  | 523.68 | 3                 | 3962.88  | 4252.28  | 631.65 | 3    | 3892.97  | 3902.06  | 528.96 |
| rc205    | 4              | 5260.14  | 5338.50  | 426.74 | 4                 | 5285.41  | 5375.54  | 221.24 | 4    | 5149.13  | 5152.79  | 368.18 |
| rc206    | 4              | 5234.55  | 5289.90  | 470.82 | 4                 | 5210.57  | 5275.72  | 395.42 | 3    | 4200.69  | 4323.33  | 517.29 |
| rc207    | 3              | 4150.60  | 4930.81  | 488.10 | 3                 | 4197.81  | 4650.01  | 607.24 | 3    | 3979.65  | 4019.57  | 490.17 |
| rc208    | 3              | 3977.50  | 4046.09  | 535.72 | 3                 | 3920.17  | 4002.79  | 527.17 | 3    | 3838.78  | 3857.49  | 457.65 |
| avg      | 8.48           | 9568.86  | 9905.20  | 435.54 | 8.18              | 9266.06  | 9479.93  | 432.20 | 7.77 | 8807.09  | 9030.14  | 262.90 |

TABLE IV  
COMPARATIVE RESULTS ON LARGE-SCALE INSTANCES IN THE JD SET WITH A SHORT TIME LIMIT.

| Instance | HMA w/o BCD |           |                   |          | HMA |           |                          |          | p-value |
|----------|-------------|-----------|-------------------|----------|-----|-----------|--------------------------|----------|---------|
|          | m           | best      | avg±std           | time     | m   | best      | avg±std                  | time     |         |
| jd200_1  | 44          | 71043.42  | 72243.96±614.67   | 1884.42  | 44  | 70979.75  | 72348.31±724.19          | 1821.75  | 0.6501  |
| jd200_2  | 39          | 59660.84  | 60785.77±551.51   | 1892.70  | 39  | 59460.27  | 60688.60±697.48          | 1825.64  | 0.7624  |
| jd200_3  | 44          | 66634.23  | 67043.56±269.90   | 1872.56  | 43  | 66254.27  | 66999.61±526.33          | 1839.70  | 0.8798  |
| jd200_4  | 39          | 60988.30  | 62033.06±488.03   | 1873.78  | 39  | 60941.60  | 61753.23±523.17          | 1843.03  | 0.2568  |
| jd400_1  | 79          | 116029.37 | 117199.07±954.98  | 5784.07  | 79  | 115981.66 | 116987.12±952.18         | 5443.33  | 0.4963  |
| jd400_2  | 77          | 116527.33 | 117584.91±736.78  | 5734.43  | 77  | 116205.05 | 117098.09±563.09         | 5430.44  | 0.1041  |
| jd400_3  | 76          | 109030.69 | 109934.10±508.53  | 5576.75  | 76  | 108441.53 | <b>109140.65±451.85</b>  | 5421.66  | 0.0032  |
| jd400_4  | 83          | 128988.11 | 129937.62±710.96  | 5761.35  | 83  | 128894.04 | 129654.11±858.13         | 5428.58  | 0.1509  |
| jd600_1  | 112         | 167369.71 | 169339.19±1098.95 | 9351.29  | 112 | 167297.70 | 168836.18±1087.42        | 9033.06  | 0.3258  |
| jd600_2  | 113         | 171996.76 | 174044.48±1610.00 | 9643.47  | 113 | 171512.97 | 173480.89±1384.65        | 9019.82  | 0.3447  |
| jd600_3  | 112         | 154336.98 | 155381.50±773.48  | 9610.60  | 111 | 153092.64 | <b>154325.16±840.34</b>  | 9037.23  | 0.0191  |
| jd600_4  | 104         | 150513.45 | 151553.99±649.75  | 9753.66  | 103 | 150123.89 | <b>150975.72±609.08</b>  | 9049.35  | 0.0343  |
| jd800_1  | 147         | 216364.67 | 217948.77±1027.41 | 13710.86 | 146 | 214710.04 | 216810.78±1542.74        | 12625.32 | 0.0757  |
| jd800_2  | 148         | 226218.76 | 228162.86±1987.21 | 13523.34 | 149 | 223610.37 | 226527.29±2364.16        | 12619.90 | 0.0963  |
| jd800_3  | 148         | 206772.88 | 208548.00±1067.70 | 13401.35 | 147 | 205215.92 | <b>207375.35±1432.89</b> | 12619.30 | 0.0494  |
| jd800_4  | 136         | 196076.58 | 197143.07±637.84  | 13603.29 | 134 | 194004.95 | 196257.28±1325.29        | 12621.05 | 0.0696  |
| jd1000_1 | 179         | 261338.90 | 262810.90±1082.93 | 17483.69 | 178 | 257410.81 | <b>260877.67±2210.64</b> | 16224.57 | 0.0343  |
| jd1000_2 | 183         | 276597.69 | 279318.78±1341.59 | 16643.43 | 184 | 274079.42 | <b>276515.30±1881.23</b> | 16224.80 | 0.0028  |
| jd1000_3 | 184         | 256229.79 | 258040.35±1467.13 | 16631.34 | 182 | 252772.63 | <b>256102.57±2369.95</b> | 16221.87 | 0.0494  |
| jd1000_4 | 169         | 243354.91 | 244808.00±1235.27 | 17552.66 | 168 | 240559.58 | <b>242952.46±2044.65</b> | 16218.06 | 0.0284  |

obtained the testing results directly from the original publications [11], [17]. To ensure a fair comparison, we rescaled the computation time to a common measure considering the CPUs used. Specifically, we rescaled the times based on the PassMark score of the CPUs used in the studies relative to our 2.60 GHz Intel Xeon Gold 6240. The PassMark score, as the performance of a single core of the respective CPU, for the 2.93 GHz X5670 used in [11], [17] is 1398, while the score of our CPU is 1990. The rescaled time in seconds is given in Tables II and III. Additionally, the run time limit on the small-scale and medium-scale instances is rescaled to 105 and 630 seconds.

Tables II and III are structured as follows. The first column lists the instance names. The “m” columns indicate the number of vehicles used in the respective solutions. For Adapt-CMSA-STD, Adapt-CMSA-SETCOV, and HMA, the “best” column refers to the  $TC$  of the best solution found in 10 independent runs, while the “avg” column refers to the average  $TC$  of the 10 runs. Finally, the “time” column shows the computation time (in seconds) for CPLEX and the average computation time for Adapt-CMSA-STD, Adapt-CMSA-SETCOV, and HMA to find the best solutions in each run, respectively. For each instance, the best performance w.r.t. “best” and “avg” are highlighted in gray, respectively.

Based on the numerical results in Table II, the following observations can be made. On small-scale instances, CPLEX, Adapt-CMSA-STD, Adapt-CMSA-SETCOV, and HMA are comparable, showing no significant difference in their best or average values due to the small solution space. Moreover, it is worth mentioning that HMA exhibits minimal computation time variation as the problem scale increases, with an average computation time of 2.20 seconds, which is much shorter than that of the other three algorithms.

Generally, the performance of algorithms on instances of

larger scales is of more interest. Overall, HMA is the best-performing algorithm on medium-scale instances as shown in Table III. In the  $r\sim$  and  $rc\sim$  subsets, the best and average solution quality obtained by HMA are consistently better than those of Adapt-CMSA-STD and Adapt-CMSA-SETCOV. Note that for the  $akb$  set, minimizing the number of the used EVs has a higher priority than minimizing  $TD$ . It is worth mentioning that HMA obtained competitive solutions with fewer EVs in 23 out of 56 instances. More specifically, these instances include 4 out of 9 in the  $cl\sim$  subset, 7 out of 12 in the  $rl\sim$  subset, 4 out of 11 in the  $r2\sim$  subset, 6 out of 8 in the  $rc1\sim$  subset, and 2 out of 8 in the  $rc2\sim$  subset. Such results indicate that HMA performed both strongly and robustly. Moreover, HMA required significantly less computation time, taking only about 60% of the time compared to the other two algorithms. In summary, the observations demonstrate that HMA outperforms all recent EVRP-TW-SPD algorithms across a broad range of problem instances, and in particular, it has significantly raised the performance bar on the  $akb$  set.

### C. Results on Large-scale Instances

To demonstrate the effectiveness of HMA for solving large-scale instances in the  $jd$  set, we limited both short and long maximum computation time and compared HMA with HMA without the BCD decomposition (denoted HMA w/o BCD). Here, we omit the existing algorithms [11], [17] for solving EVRP-TW-SPD because they are not open-sourced. Specifically, instances with 200, 400, 600, 800, and 1000 customers were decomposed into 2, 4, 6, 8, and 10 subproblems in the MS of HMA (see Algorithm 3). The short time limits were set to 1800, 5400, 9000, 12600, and 16200 seconds (see Table IV), while the long time limits were 3600, 10800, 18000, 25200, and 32400 seconds (see Table V). Note that BCD requires the Cartesian coordinate of node  $n_i$ , while the  $jd$  set contains lon-

TABLE V  
COMPARATIVE RESULTS ON LARGE-SCALE INSTANCES IN THE JD SET WITH A LONG TIME LIMIT.

| Instance | HMA w/o BCD |           |                   |          | HMA |           |                          |          | p-value |
|----------|-------------|-----------|-------------------|----------|-----|-----------|--------------------------|----------|---------|
|          | m           | best      | avg±std           | time     | m   | best      | avg±std                  | time     |         |
| jd200_1  | 44          | 70740.90  | 71335.98±403.87   | 3678.82  | 44  | 70440.57  | 71409.68±512.27          | 3510.36  | 0.6501  |
| jd200_2  | 39          | 59389.70  | 60004.86±419.68   | 3661.48  | 38  | 58530.22  | 59823.10±570.84          | 3612.10  | 0.3643  |
| jd200_3  | 42          | 65201.82  | 65844.88±445.08   | 3544.28  | 43  | 65812.71  | 66206.45±284.52          | 3534.71  | 0.0588  |
| jd200_4  | 39          | 60747.28  | 60983.75±250.76   | 3571.75  | 39  | 60815.01  | 61008.17±184.95          | 3362.58  | 0.4497  |
| jd400_1  | 78          | 114537.34 | 116518.79±1422.92 | 10492.89 | 78  | 114489.28 | 115579.17±715.05         | 10474.83 | 0.1306  |
| jd400_2  | 76          | 115303.21 | 116803.18±612.69  | 10409.36 | 77  | 114668.85 | <b>115658.43±606.08</b>  | 10815.96 | 0.0015  |
| jd400_3  | 76          | 106951.59 | 107842.05±588.35  | 10547.36 | 76  | 107600.70 | 107927.90±351.95         | 10063.53 | 0.8206  |
| jd400_4  | 81          | 126613.16 | 127573.34±914.21  | 10687.95 | 82  | 126927.71 | 127814.74±492.32         | 10362.35 | 0.2265  |
| jd600_1  | 112         | 166524.71 | 168729.52±1110.96 | 14626.36 | 112 | 166113.91 | <b>166952.86±681.25</b>  | 18016.97 | 0.0019  |
| jd600_2  | 113         | 171996.76 | 173256.93±1387.16 | 14450.07 | 113 | 170362.24 | <b>171446.42±618.81</b>  | 17416.13 | 0.0007  |
| jd600_3  | 110         | 151879.40 | 153745.61±1118.40 | 16444.28 | 109 | 151185.33 | <b>152554.96±942.57</b>  | 17806.93 | 0.0494  |
| jd600_4  | 103         | 149893.97 | 151118.39±658.62  | 13495.48 | 103 | 148729.43 | <b>149447.53±563.44</b>  | 17432.51 | 0.0004  |
| jd800_1  | 147         | 216194.15 | 217442.46±805.04  | 20030.45 | 146 | 213065.47 | <b>214228.94±974.71</b>  | 25217.34 | 0.0002  |
| jd800_2  | 148         | 226218.76 | 227630.94±1710.11 | 19306.58 | 147 | 222333.51 | <b>223685.24±1338.04</b> | 25214.00 | 0.0007  |
| jd800_3  | 147         | 205429.64 | 207285.21±1202.21 | 23965.29 | 146 | 203751.04 | <b>205483.36±1355.49</b> | 24410.31 | 0.0082  |
| jd800_4  | 135         | 194738.56 | 196802.01±952.89  | 23059.46 | 134 | 192848.13 | <b>194144.22±987.70</b>  | 24949.64 | 0.0005  |
| jd1000_1 | 178         | 260502.17 | 262307.88±1199.71 | 29046.07 | 178 | 256626.16 | <b>257932.03±1114.15</b> | 32159.10 | 0.0002  |
| jd1000_2 | 182         | 275972.37 | 278824.43±1564.13 | 28589.01 | 181 | 270788.78 | <b>273195.12±1537.57</b> | 32421.83 | 0.0002  |
| jd1000_3 | 184         | 256229.79 | 257553.76±1262.58 | 25397.05 | 181 | 250802.03 | <b>253040.02±1411.33</b> | 31452.40 | 0.0002  |
| jd1000_4 | 169         | 242662.53 | 244305.00±1250.99 | 27539.25 | 167 | 238562.78 | <b>239966.65±1244.47</b> | 32276.48 | 0.0002  |

gitude and latitude. Since the area covered is not large, we can use Mercator Projection to convert  $(lng_i, lat_i)$  into  $(x_i, y_i)$ , specifically,  $x_i = R \cdot \frac{\pi \cdot lng_i}{180}$ ,  $y_i = R \cdot \ln\left(\tan\left(\frac{\pi}{4} + \frac{\pi \cdot lat_i}{360}\right)\right)$ , where  $R$  is the semi-major axis of the WGS84 ellipsoid model. In Tables IV and V, the “avg±std” columns represent the average and standard deviation of  $TC$  for the 10 best solutions found in 10 independent runs. We used the Wilcoxon rank-sum test with significance level  $p = 0.05$  to compare the performance of HMA w/o BCD and HMA, with p-values shown in the last column. The best performance w.r.t. “best” is highlighted in gray, and w.r.t. “avg±std” is highlighted in bold if it is significantly better than the other algorithm, respectively.

From Table IV, it can be observed that under a short time limit, HMA consistently found better solutions on all instances of the  $jd$  set compared to HMA w/o BCD. The average performance of HMA is significantly better as the problem scale increases. In Table V, under a long time limit, HMA w/o BCD performed reversely better on some instances with 200 and 400 customers. This is due to the challenge of designing an ideal decomposition, which would partition all customers belonging to the same route in the optimal solution into the same subproblem. However, other decompositions, such as BCD, solve subproblems efficiently but may result in suboptimal solutions. Nonetheless, as the problem scale grows, the decomposition strategy still shows an obvious advantage on instances of larger scale with 600, 800, and 1000 customers since HMA obtained significantly higher-quality solutions. The performance gap between HMA w/o BCD and HMA across 10 independent runs, measured as  $[TC_1 - TC_2]/TC_2$ , where  $TC_1$  and  $TC_2$  are the value of best-found solutions from HMA w/o BCD and HMA, is 0.61%, 1.26%, and 1.83% averaged on instances with 600, 800, and 1000 customers, respectively. As the problem scale grows, the performance gap

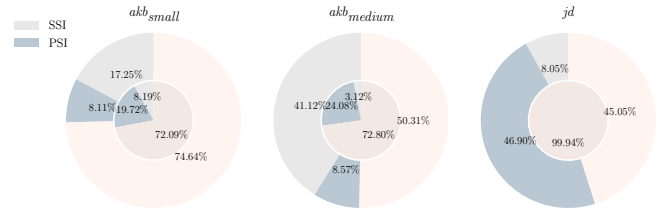


Fig. 2. Comparative effects of PSI and SSI on each subset. The outer ring represents the exclusive contribution ratio (ECR) of SSI and PSI, with the remainder being shared contributions; The inner ring shows the time allocation ratio (TAR) of SSI and PSI, with the remainder representing others’ TAR.

between HMA w/o BCD and HMA also becomes larger.

#### D. Effectiveness of PSSI, CDNS, and Hybrid Framework

First, we separately analyzed the comparative effects of PSI and SSI for the following reasons: PSSI selects the best result from PSI and SSI. Therefore, we are more concerned about which strategy, PSI or SSI, achieves better station insertion on a route. Note that SSI produces only a single route, compared to PSI with a population. We need to validate whether PSSI can really find other higher-quality station insertion configurations with acceptable additional computational cost. To this end, we ran HMA once on all instances, keeping track of the performance of PSI and SSI in terms of station insertion on the same route. Figure 2 presents the performance of PSI and SSI: the exclusive contribution ratio (ECR) is computed as  $n_1/n_2$  for each instance, where  $n_1$  is the number of insertion results obtained exclusively from SSI or PSI and  $n_2$  is the total number of insertion results; the time allocation ratio (TAR) is computed as  $t_1/t_2$  for each instance, where  $t_1$  is the cumulative time consumed in SSI or PSI components,  $t_2$  is the total time consumed in HMA. Note that the outer ring “ECR”

TABLE VI  
AVERAGE PDR FOR THE FOUR HMA VARIANTS ON EACH SUBSET.

| Subset         | w/o CLS | w/o ALS | w/o MS | w/o LNS |
|----------------|---------|---------|--------|---------|
| $akb_{small}$  | 1.80%   | 0.00%   | 2.94%  | 0.00%   |
| $akb_{medium}$ | 1.03%   | 0.06%   | 3.49%  | 0.37%   |
| $jd$           | 0.00%   | 4.03%   | 0.60%  | 2.47%   |
| Avg.PDR        | 0.84%   | 0.77%   | 2.98%  | 0.75%   |

and inner ring “TAR” in Figure 2 are the average values on each subset.

From the results, it can be clearly seen that PSI can really find other higher-quality station insertions, as  $ECR > 0$  indicates that it found some strictly better insertions than SSI. In the  $jd$  set, the ECR of PSI even achieved 46.90%, accounting for a large proportion of contributions to PSSI. Notably, although PSI with a genetic algorithm took approximately 2 ~ 8 times runtime than SSI, this additional runtime is worthwhile and acceptable, as SSI cannot further improve its insertion results. Thus, combining the results of both PSI and SSI can better avoid local optima and construct higher-quality routes with acceptable additional computational cost.

Second, we conducted an ablation study to evaluate the effectiveness of other components in HMA. We tested the following four variants on the  $akb$  and  $jd$  sets, each of which is different from HMA in one component:

- 1) w/o CLS: lines 11-13 of Algorithm 2 are removed;
- 2) w/o ALS: lines 1-10 of Algorithm 2 are removed;
- 3) w/o MS: lines 9-19 of Algorithm 3 are removed;
- 4) w/o LNS: lines 2-7, 22-23 of Algorithm 3 are removed.

The first two variants were to validate the effectiveness of CDNS, while the latter two were to validate the effectiveness of the hybrid framework. For each variant, the performance degradation ratio (PDR) is computed as  $[TC_1 - TC_2]/TC_2$  for each instance, where  $TC_1$  and  $TC_2$  are the average  $TC$  obtained by the variant and HMA across 10 independent runs, respectively.  $PDR > 0$  indicates the component is useful for this specific instance. Larger values indicate a greater impact. Table VI presents the average PDR on each subset.

The results show that, on average, no component negatively affects the performance of HMA. Specifically, the “w/o CLS” and “w/o ALS” results show that CLS benefits small-scale and medium-scale instances, while ALS is more effective for large-scale instances. CLS is good at refined search, which is beneficial for small solution spaces. In contrast, ALS leverages existing efficient VRP-TW-SPD move evaluation, advantageous for large solution spaces that require fast exploration. Similarly, the “w/o MS” and “w/o LNS” results indicate that MS is more effective for small-scale and medium-scale instances due to population diversity, whereas a fast search of LNS benefits large-scale instances. The population maintains solution diversity in smaller problems; however, as the problem scale increases, the dominant role of individual-based search capabilities becomes more evident.

## VI. CONCLUSION

This work investigated an emerging routing problem, namely EVRP-TW-SPD, and proposed a hybrid memetic algorithm called HMA to solve it. HMA integrates two novel components: PSSI for handling partial recharges and CDNS as the local search procedure. Both components can be easily applied to other EVRP variants. Comprehensive experiments showed that HMA outperformed existing methods across a wide range of instances. Moreover, a new, large-scale benchmark set was established from a real-world JD logistics application. This set contains 20 problem instances with 200, 400, 600, 800, and 1000 customers, each with 100 stations,

HMA can be further improved in several directions. First, the PSSI procedure could benefit from a learned function (e.g., as a neural network [35]) that evaluates insertions instead of heuristic rules, which might lead to higher-quality feasible routes within even smaller time budget. Second, dividing the original problem into smaller, manageable subproblems enhances efficiency and yields high-quality solutions. However, the success of this approach heavily depends on the effectiveness of the decomposition strategy. Rather than relying on hand-designed strategies, future improvements could leverage learning-based methods [36] or general-purpose pretrained models [37] to automatically design effective decomposition strategies tailored to specific customer distributions.

### APPENDIX A PROOF OF PROPOSITION 1

**Proof.** Consider a feasible EVRP-TW-SPD solution  $\mathcal{S}$ . By definition,  $\mathcal{S}$  satisfies all electricity, capacity, and time window constraints. Let  $\bar{\mathcal{S}}$  be the solution obtained by removing all charging stations in  $\mathcal{S}$ . Suppose the travel time between any two nodes satisfies the triangle inequality, then for any two successive customers  $c_i$  and  $c_j$  in  $\bar{\mathcal{S}}$  that are separated by a charging station  $f$ , the triangle inequality ensures:

$$t_{c_i c_j} \leq t_{c_i f} + t_{f c_j} + g \cdot q_f,$$

where  $g \cdot q_f$  is the charging time at station  $f$ . This inequality implies that the travel time between customers in  $\bar{\mathcal{S}}$  is no greater than in  $\mathcal{S}$ . Consequently,  $\bar{\mathcal{S}}$  satisfies all capacity and time window constraints of VRP-TW-SPD, making it a feasible solution.

In cases where the travel time does not satisfy the triangle inequality, we can preprocess the problem instance to ensure this property holds. Specifically, we first apply the Floyd-Warshall algorithm to compute the shortest path in terms of travel time between every pair of nodes. These shortest paths are allowed to pass through charging stations but not through the depot or other customers. We then reconstruct the edge set  $\mathcal{E}$  using these shortest paths, defining each new edge (or “hyperarc”) as  $(i, j)$  to be the shortest path from node  $i$  to  $j$ . The travel time associated with these new edges naturally satisfies the triangle inequality, allowing Proposition 1 to hold for any problem instance.  $\square$

## REFERENCES

- [1] X. Wen, G. Wu, J. Liu, and Y.-S. Ong, "Transfer optimization for heterogeneous drone delivery and pickup problem," *IEEE Trans. Emerg. Top. Comput. Intell.*, pp. 1–18, 2024.
- [2] L. Feng, Y. Huang, L. Zhou, J. Zhong, A. Gupta, K. Tang, and K. C. Tan, "Explicit evolutionary multitasking for combinatorial optimization: A case study on capacitated vehicle routing problem," *IEEE Trans. Cybern.*, vol. 51, no. 6, pp. 3143–3156, 2021.
- [3] M. Chen, J. Chen, P. Peng, S. Liu, and K. Tang, "A heuristic repair method for dial-a-ride problem in intracity logistic based on neighborhood shrinking," *Multimed. Tools Appl.*, vol. 80, no. 20, pp. 30775–30787, 2021.
- [4] J. Mandziuk, "New shades of the vehicle routing problem: Emerging problem formulations and computational intelligence solution methods," *IEEE Trans. Emerg. Top. Comput. Intell.*, vol. 3, no. 3, pp. 230–244, 2019.
- [5] H. Qin, X. Su, T. Ren, and Z. Luo, "A review on the electric vehicle routing problems: Variants and algorithms," *Front. Eng. Manag.*, vol. 8, pp. 370–389, 2021.
- [6] Z. Zhou, B. Wang, Y. Guo, and Y. Zhang, "Blockchain and computational intelligence inspired incentive-compatible demand response in internet of electric vehicles," *IEEE Trans. Emerg. Top. Comput. Intell.*, vol. 3, no. 3, pp. 205–216, 2019.
- [7] Y. Liu, P. Zhou, L. Yang, Y. Wu, Z. Xu, K. Liu, and X. Wang, "Privacy-preserving context-based electric vehicle dispatching for energy scheduling in microgrids: An online learning approach," *IEEE Trans. Emerg. Top. Comput. Intell.*, vol. 6, no. 3, pp. 462–478, 2022.
- [8] S. Erdoğan and E. Miller-Hooks, "A green vehicle routing problem," *Transp. Res. Part E Logist. Transp. Rev.*, vol. 48, no. 1, pp. 100–114, 2012.
- [9] I. Küçükoglu, R. Dewil, and D. Cattrysse, "The electric vehicle routing problem and its variations: A literature review," *Comput. Ind. Eng.*, vol. 161, p. 107650, 2021.
- [10] C. Wang, M. Cao, H. Jiang, X. Xiang, and X. Zhang, "A deep reinforcement learning-based adaptive large neighborhood search for capacitated electric vehicle routing problems," *IEEE Trans. Emerg. Top. Comput. Intell.*, pp. 1–14, 2024.
- [11] M. A. Akbay, C. B. Kalayci, and C. Blum, "Application of CMSA to the electric vehicle routing problem with time windows, simultaneous pickup and deliveries, and partial vehicle charging," in *Proceedings of MIC'2022*, Syracuse, Italy, Jul 2022, pp. 1–16.
- [12] M. Schneider, A. Stenger, and D. Goetze, "The electric vehicle-routing problem with time windows and recharging stations," *Transp. Sci.*, vol. 48, no. 4, pp. 500–520, 2014.
- [13] J. Dethloff, "Vehicle routing and reverse logistics: The vehicle routing problem with simultaneous delivery and pick-up," *OR Spectr.*, vol. 23, no. 1, pp. 79–96, 2001.
- [14] N. A. Wassan, A. H. Wassan, and G. Nagy, "A reactive tabu search algorithm for the vehicle routing problem with simultaneous pickups and deliveries," *J. Comb. Optim.*, vol. 15, no. 4, pp. 368–386, 2008.
- [15] M. Keskin and B. Çatay, "Partial recharge strategies for the electric vehicle routing problem with time windows," *Transp. Res. Part C Emerg. Technol.*, vol. 65, pp. 111–127, 2016.
- [16] G. Desaulniers, F. Errico, S. Irnich, and M. Schneider, "Exact algorithms for electric vehicle-routing problems with time windows," *Oper. Res.*, vol. 64, no. 6, pp. 1388–1405, 2016.
- [17] M. A. Akbay, C. Blum, and C. B. Kalayci, "Cmsa algorithms for the electric vehicle routing problem with simultaneous pickup and deliveries, time windows and partial battery charging," 2023, available at SSRN: <http://dx.doi.org/10.2139/ssrn.4459937>.
- [18] F. Feng, B. Qian, R. Hu, N. Yu, and Q. Shang, "ADMM with SUSLM for electric vehicle routing problem with simultaneous pickup and delivery and time windows," in *Proceedings of ICIC'2023*, Zhengzhou, China, Aug 2023, pp. 15–24.
- [19] S. Liu, K. Tang, and X. Yao, "Memetic search for vehicle routing with simultaneous pickup-delivery and time windows," *Swarm Evol. Comput.*, vol. 66, p. 100927, 2021.
- [20] W. Wang and J. Zhao, "Partial linear recharging strategy for the electric fleet size and mix vehicle routing problem with time windows and recharging stations," *Eur. J. Oper. Res.*, vol. 308, no. 2, pp. 929–948, 2023.
- [21] M. Keskin and B. Çatay, "A matheuristic method for the electric vehicle routing problem with time windows and fast chargers," *Comput. Oper. Res.*, vol. 100, pp. 172–188, 2018.
- [22] M. Keskin, B. Çatay, and G. Laporte, "A simulation-based heuristic for the electric vehicle routing problem with time windows and stochastic waiting times at recharging stations," *Comput. Oper. Res.*, vol. 125, p. 105060, 2021.
- [23] G. Berbeglia, J.-F. Cordeau, I. Gribkovskaia, and G. Laporte, "Static pickup and delivery problems: a classification scheme and survey," *Top.*, vol. 15, pp. 1–31, 2007.
- [24] Ç. Koç, G. Laporte, and I. Tükenmez, "A review of vehicle routing with simultaneous pickup and delivery," *Comput. Oper. Res.*, vol. 122, p. 104987, 2020.
- [25] K. Tang, S. Liu, P. Yang, and X. Yao, "Few-shots parallel algorithm portfolio construction via co-evolution," *IEEE Trans. Evol. Comput.*, vol. 25, no. 3, pp. 595–607, 2021.
- [26] H. Min, "The multiple vehicle routing problem with simultaneous delivery and pick-up points," *Transp. Res. Part A: Gen.*, vol. 23, no. 5, pp. 377–386, 1989.
- [27] F. A. T. Montané and R. D. Galvão, "Vehicle routing problems with simultaneous pick-up and delivery service," *Opsearch*, vol. 39, pp. 19–33, 2002.
- [28] Y. Gajpal and P. L. Abad, "Saving-based algorithms for vehicle routing problem with simultaneous pickup and delivery," *J. Oper. Res. Soc.*, vol. 61, no. 10, pp. 1498–1509, 2010.
- [29] H. Mao, J. Shi, Y. Zhou, and G. Zhang, "The electric vehicle routing problem with time windows and multiple recharging options," *IEEE Access*, vol. 8, pp. 114864–114875, 2020.
- [30] J. Lu, "Study on distribution path planning of electric logistics vehicles under partial charging strategy," *Acad. J. Sci. Technol.*, vol. 10, no. 1, pp. 202–210, 2024.
- [31] R. Roberti and M. Wen, "The electric traveling salesman problem with time windows," *Transp. Res. Part E Logist. Transp. Rev.*, vol. 89, pp. 32–52, 2016.
- [32] Á. Felipe, M. T. Ortuño, G. Righini, and G. Tirado, "A heuristic approach for the green vehicle routing problem with multiple technologies and partial recharges," *Transp. Res. Part E Logist. Transp. Rev.*, vol. 71, pp. 111–128, 2014.
- [33] A. Santini, M. Schneider, T. Vidal, and D. Vigo, "Decomposition strategies for vehicle routing heuristics," *INFORMS J. Comput.*, vol. 35, no. 3, pp. 543–559, 2023.
- [34] S. Salhi and G. Nagy, "A cluster insertion heuristic for single and multiple depot vehicle routing problems with backhauling," *J. Oper. Res. Soc.*, vol. 50, no. 10, pp. 1034–1042, 1999.
- [35] S. Liu, Y. Zhang, K. Tang, and X. Yao, "How good is neural combinatorial optimization? A systematic evaluation on the traveling salesman problem," *IEEE Comput. Intell. Mag.*, vol. 18, no. 3, pp. 14–28, 2023.
- [36] K. Tang and X. Yao, "Learn to optimize—a brief overview," *Natl. Sci. Rev.*, p. nwae132, 2024.
- [37] S. Liu, C. Chen, X. Qu, K. Tang, and Y.-S. Ong, "Large language models as evolutionary optimizers," in *Proceedings of the IEEE CEC'2024*, Yokohama, Japan, Jun 2024, pp. 1–8.